Original Paper

Deformation Behavior of Corrugated Medium During Wedge Indentation into Heightwise Corrugated

Shigeru NAGASAWA[*†], Masatoshi FUJIKURA[*]
Yasushi FUKUZAWA[*] and Takashi KAJIZUKA[**]

This paper describes the occurrence phenomena of string-like paper dust on the die-cutting process of corrugated paperboard (Cpb). In order to reveal the effect of blade position from the apex of a corrugated medium (CM) on the deformation behavior of the CM, a cutting blade was quasi-statically indented to Cpb and the side view of Cpb was observed by using a CCD camera. Through this experiment, the followings were revealed. (1) Deformation behavior of the CM during the blade indentation was classified into three macro groups: M-like form (apex crushing), Z-like form (doubly-folded), and W-like form (back-side liner and root crushing). (2) Z-like form was subdivided into the three modes C, D, and E; representing the blade moved aside a Z-form due to insufficient folding; the blade just cut off the Z-form, and the blade moved aside the Z-form due to surplus folding, respectively. Five or three modes were arranged for a half range (in the right or the left) on the setup position X of the blade. (3) Asymmetric structure of the CM wave affects the distribution of deformation modes of the CM with respect to X. (4) Constraint of Cpb affects the occurrence probability of deformation modes.

Keywords : shear, die cutting, inner flute, blade position, folding, thread-like dust

1. Introduction

In the production process of packaging containers, which are composed of corrugated paperboards (Cpb) and/or coated paperboards, the flatbed (the platen) die-cutter is generally used for cutting off work sheets[1, 2]. Since the pattern development of packaging containers made by Cpb is normally standardized in various markets, the same steel-rule die is apt to be used for a long cutting duration, more than hundreds of thousands of times, but less than one million times. Therefore, the durability of cutting tools and the quality of sheared profiles of work sheets are important for advanced production technology of packaging containers. It is necessary to consider corrective action on the paper dust to solve any problem that may occur in the pre/main/post processing of a flatbed die-cutting.

In order to clean up and reduce the paper dusts, setup of dust collectors and manual sweeping actions by human hands are usually considered. Adding this, brief stops of the flatbed die-cutter are also necessary for inspecting the quality of die-cutting. Regarding this problem, when a cutting blade (wedge) is indented to an inner liner stacked on a heightwise corrugated medium (CM), it is empirically known that the

[*] Nagaoka University of Technology, Dept. of Mechanical Eng.,
** Rengo Co. Ltd., Packaging Technical Center,
†Corresponding author, 1603-1 Kamitomioka, Nagaoka, Niigata 940-2188, Japan, Tel/Fax: +81-258-47-9701,
Email: snaga@mech.nagaokaut.ac. jp

CM is deformed into Z-like crushed structure. And the string-like paper dusts are sometimes generated from the cutting process of the Z-like crushed CM[3]. Collected paper dusts actually include powder-like fine dusts, sliced chips, and string-like (or thread-like) dusts.

The frequency of occurrence of paper dusts appears to vary with the processing style, depending on whether it is the flatbed type or the rotary type die-cutter[2]. Furthermore, there appear to be several causes corresponding to each form (profile) of the paper dusts, in the flatbed type or in the rotary type. In order to develop any corrective actions, it is necessary to investigate the occurrence mechanism of paper dusts.

In this study, therefore, the occurrence of Z-like crushed CM was statistically investigated when the rectangle-formed specimen of heightwise Cpb was quasi-statically subjected to indentation of a 42° center-bevelled blade (virgin straight knife) by varying the blade position from the apex position of the CM wave. In this process, the side view of Cpb was observed by using a CCD camera in order to reveal the effect of blade position on the deformation behavior of the CM.

2. Experimental

2.1 Specimens

Fig. 1 shows the size of a specimen formed in a rectangle. The specimen was made of a C-fluted board, which was composed of the inner liner, the outer liner and the CM. Nominal specification was as follows: height of Cpb: t= 4.0 /mm, wave length of the CM: λ= 7.9 /mm; basis weight of the liners: 170 /gm^{-2}; thickness of the liners: 0.2 /mm; basis weight of the CM: 120 /gm^{-2} and thickness of the CM: 0.2 /mm.

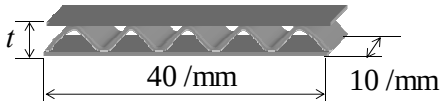

Fig.1 Layout and size of specimen

Table1 In-plane tensile properties of specified raw-material sheets (strain rate:0.28×10^{-3}/s^{-1})

Raw-material sheets	Young's modulus /GPa	Ult. Tens. Strength /MPa	Breaking strain %
Liner (MD)	5.51(0.13)	56.7 (1.69)	2.0 (0.12)
Liner (CD)	1.64(0.20)	21.1 (0.77)	5.2 (0.41)
Corrugated medium (MD)	4.07(0.24)	31.7 (1.39)	1.5 (0.14)
Corrugated medium (CD)	1.22(0.09)	11.1 (0.40)	2.3 (0.29)

Average (standard deviation) for 10 samples

The in-plane mechanical properties, based on the JIS-P-8113 tensile testing, of the liners and the CM are shown in Table 1. Here, MD: Machine direction, CD: Cross machine direction. Specimens of Cpb were prepared in a room at an average temperature of 296 K and humidity of 50%RH for 24 hours.

2.2 Experimental condition

Fig.2 shows the schematics of the experimental apparatus. The upper crosshead had the cutting-blade mounted on a load cell with the maximum loading capacity of 10 /kN. Fig.2 (a) shows the structural relation between the lower counter plate (copper) and the work sheet (Cpb) subjected to a pushing load by the blade, while Fig.2 (b) shows the setup position e of the blade from the apex position of the CM wave. Displacement of the blade was controlled by a servo actuator CYP-3-10 (Shinto Kogio) with the position accuracy of +/–0.01 /mm.

The front (outside) liner of the work sheet was attached to the lower counter plate, the groove of which has the depth of 1 /mm and the length of 40.5 /mm. The work sheet was fixed at the height of 4.0 /mm by using a pair of retainer plate in order to restrict softly the bend-up of the work sheet. This constraint was here defined as the *soft-fixing* condition. In order to confirm the effect of *soft-fixing* JIG, another plain counter plate (without step-like groove) was prepared, and the retainer plates were removed. This constraint was defined as the *free* condition.

The high-carbon steel (SK5) blade[4] had the following specification: tip hardness of 690 VHN, apex angle α of 42°, tip thickness w of 5 /μm, body thickness of 0.71 /mm, length of 40 /mm, and peaking height of the blade 5.6 /mm.

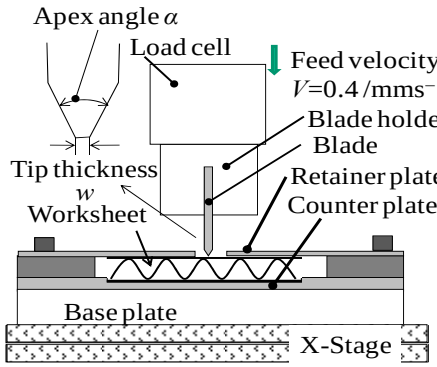

(a) Structure of blade, lower plate and X-stage

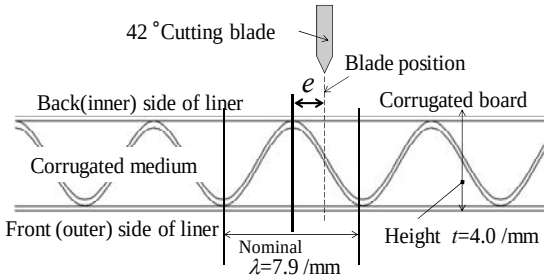

(b) Details of blade position and work sheet

Fig.2 Schematics of cutting apparatus

The heightwise flute of the work sheet was adjusted for being parallel to the cutting-blade by using the CCD camera (Keyence digital microscope VHX-200, VH-Z35, picture element: 2,110,000 pixel), and the lower base plate was secondly moved for adjusting the setup position e of the blade by using the X-stage. On the experiment apparatus, the upper crosshead moved downward with a feed velocity V of 0.4 /mms^{-1}. Indentation depth d of the blade was measured by a displacement meter of the servo actuator CYP-3-10 until the outside liner (lower liner) was cut off, while the cutting force F /kN (= specimen width L x line force f /kNm^{-1}) of the blade was measured using the load cell.

Normalized setup position $X=e/\lambda$ of the blade was chosen from −0.5 up to +0.5. Here, X=0 corresponded to the condition under which the blade was manually set to the middle position of the CM wave (on a middle line of the height of Cpb). The CCD camera was used for recording video images as shown in Fig.3, in order to observe the deformation flow in the side view of the work sheet during the blade indentation. The *free* condition of the work sheet is illustrated in Fig.3. Sample numbers were 10 for each setup position X of the blade.

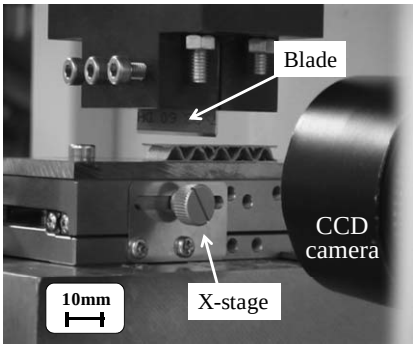

Fig.3 Observation unit and cutting apparatus (in case of *free* condition)

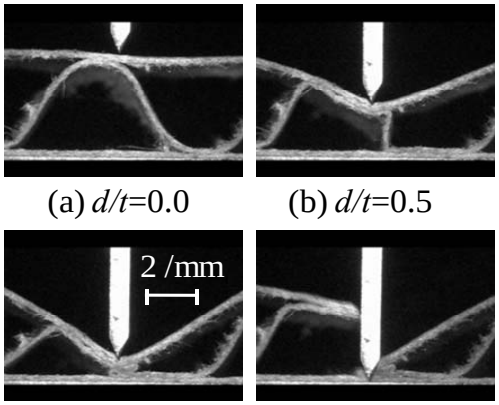

(a) d/t=0.0 (b) d/t=0.5

(c) d/t=0.8 (d) d/t=1.0

Fig.4 Video photographs of side view of C-fluted board during blade indentation (Z-like crushing in case of X= +0.1)

3. Results and discussion

3.1 Deformation modes of CM

Fig.4 shows an example of sectional-view photographs of the C-fluted board subjected to blade indentation at the setup position of X= +0.1 for d/t= 0~1.0. This deformation flow was recognized as the Z-like crushing mode from Fig.4 (c). All the deformation behavior of the CM was classified with respect to the crushing modes during d/t= 0.5~1.0 from the video images.

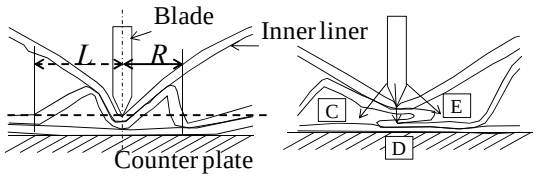

(a) M-like crushing (b) Z-like crushing

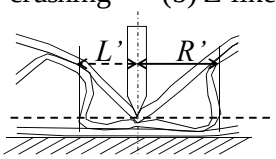

(c) W-like crushing

Fig.5 Three-classified deformation modes of corrugated medium subjected to a wedge indentation by varying setup position of blade (in case of $0<X<0.5$)

The occurrence of Z-like form and the occurrence of string-like dust were statistically observed for d/t= 0.8~1.0. Through this observation of the crushed CM, the next three deformation modes, as shown in Fig.5, were found as the macro group: (i) M-like form (apex crushing), (ii) Z-like form (doubly-folded), and (iii) W-like form (back-side liner and root crushing). When d/t=0.8, the distance L, R or L', R' were measured from the video images as shown in Fig.5. Here, those parameters were defined as the distance between the blade position and the cross points of the CM with the level of d/t= 0.8. Using the ratio of L/R or L'/R', all deformation modes were classified to be of seven kinds as A, B+, C+, D+, E+, F+, G+ for $0 \leqq X \leqq 0.5$, as shown in Table 2. The plus symbol meant that the crushing occurred at the right-half zone: $0 \leqq X \leqq 0.5$. Similarly, denoting the minus symbol as the left-half zone: $-0.5 \leqq X < 0$, deformation modes were of six kinds as B–, C–, D–, E–, F–, G–. Here, G+ is the same as G– due to the periodicity of the CM wave.

Table 2 Deformation modes of corrugated medium (13 kinds of branched state)

Mode(+)	A	B+	C+	D+	E+	F+	G+
$0.5 \geqq X \geqq 0$	L/R =1	L/R >1	Fall in the left	Just cut on the Z	Fall in the right	L'/R' <1	L'/R' =1
Mode(-)		**B–**	**C–**	**D–**	**E–**	**F–**	**G–**
$0>X \geqq -0.5$		L/R <1	MRR of C+	Just cut on the Z	MRR of E+	L'/R' >1	L'/R' =1

Since the deformation of the CM with A and G(+/–) was perfectly symmetric, the occurrence of those states was not observed actually. Therefore, only 10 kinds of deformation modes B (+/–), C (+/–), D (+/–), E (+/–), F (+/–) were actually observed in the range of $-0.5 \leqq X \leqq$

0.5.

When the CM of the work sheet was crushed in Z-like form for d/t <0.8, the crushed form of the CM branched to three deformation modes in the final state: C, D and E. In the case of Mode D(+/–), the blade just cut off the doubly-folded CM (Z-like form) and then two pieces of string-like dust were normally generated, although a piece of string-like dust was sometimes generated when the one folded part dynamically escaped from biting of the blade tip.

Fig.6 shows an example of string-like dust occurred at Mode D+. A folded strip with a width of 1 /mm was detected as the string-like dust. In the case of Mode C or E, the blade moved aside the doubly-folded part without cutting off the CM. All the modes defined in Table 2 were synthetically arranged as follows: M-like form includes A, B(+/–); Z-like form includes C(+/–), D(+/–), E(+/–); and W-like form includes F(+/–), G(+/–), respectively.

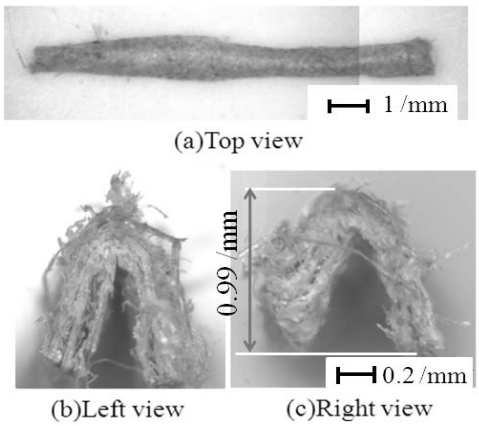

Fig.6 Example of string-like dust occurred at Mode D+

3.2 Occurrence frequency of crushing form with fixing condition

Through the experiment, the occurrence of Z-like form appeared in the range of $0.3>X>-0.4$ in both the *soft-fixing* and *free* conditions. Fig.7 shows the occurrence frequency of the deformation modes B, D, F and the union mode {C,D,E} in the case of the *soft-fixing* constraint. Fig.8 shows the distribution of frequency of the macro-grouped modes (Z, M, W-like form) with respect to the setup position of the blade $X= e/\lambda$, in the case of the *soft-fixing* constraint. Similarly, Fig.9 shows the occurrence frequency of deformation modes B, D, F and the union mode {C,D,E} in the *free* condition case. Fig.10 shows the distribution of frequency of the macro-grouped modes (Z, M, W-like form) in the *free* condition case.

From Figs.7 to 10, the following features were revealed: (i) Distribution of occurrence frequency of the deformation modes B, C, D, E, F was statistically asymmetric concerning the setup position of the blade X. (ii) In the case of the *free* condition, both the distribution of M-like and W-like form tended to scatter widely with respect to X, as compared to the *soft-fixing* constraint. (iii) Distribution of the occurrence frequency of the union mode {C, D, E} was varied with the boundary constraint. (iv) M-like form tended to occur at the range of $|e| < \lambda/4$.

Due to the periodicity of the CM wave, Table 3 shows the estimated probability of representative modes for $-0.5<X<0.5$. Here, the probability p_i of Mode i was estimated from Eq.(1), by using the frequency ρ_i occurred at X with Mode i (= B,C,D,E,F and so on).

$$p_i = \int_{-0.5}^{0.5} \rho_i(X)dX \qquad \text{Eq.(1)}$$

From the experiment, since $\rho_A = \rho_G = 0$ for $-0.5 < X < 0.5$, the union {A,B} was the same as Mode B, and also the union {F,G} was the same as Mode F in Table 3.

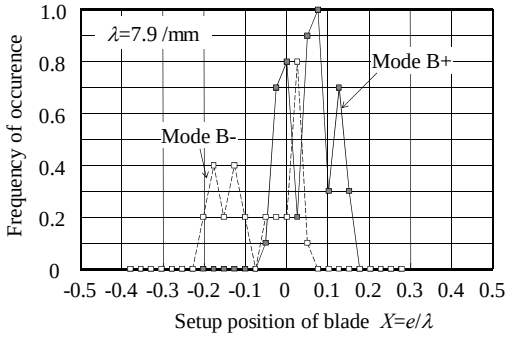

(a) In case of Mode B+ and B-

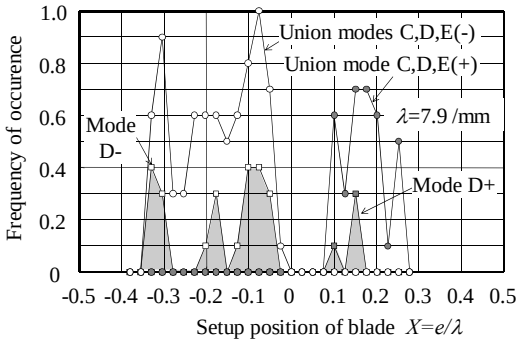

(b) In case of Mode D+, D- and Union modes of C, D, E (+/-)

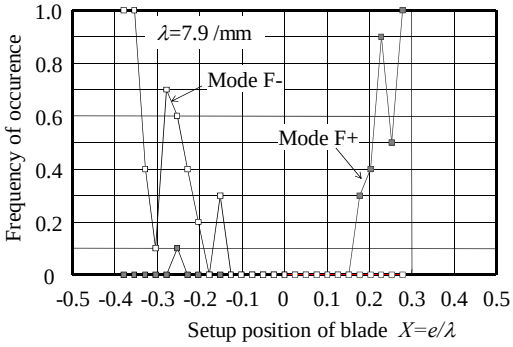

(c) In case of Mode F+ and F-

Fig.7 Distribution of deformation modes occurred at d/t=0.8 with soft-fixing constraint (10 samples for each X measured)

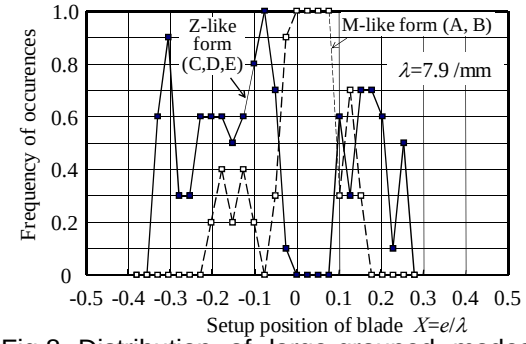

Fig.8 Distribution of large-grouped modes: Z-like and M-like crushing form with soft-fixing constraint

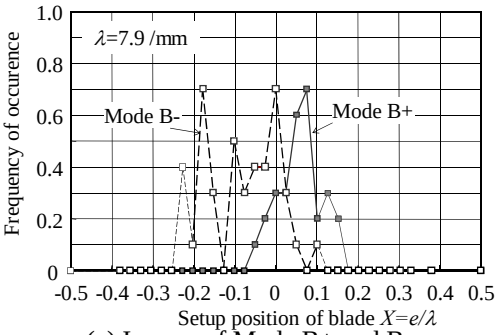

(a) In case of Mode B+ and B-

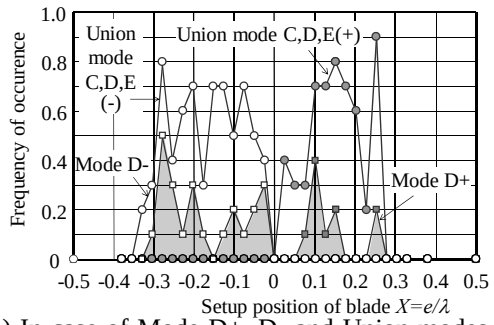

(b) In case of Mode D+, D- and Union modes of C, D, E (+/-)

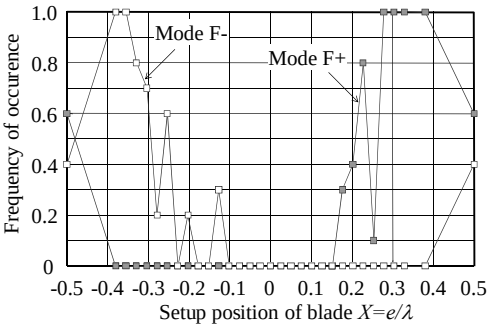

(c) In case of Mode F+ and F-

Fig.9 Distribution of deformation modes occurred at d/t=0.8 with free condition (10 samples for each X measured)

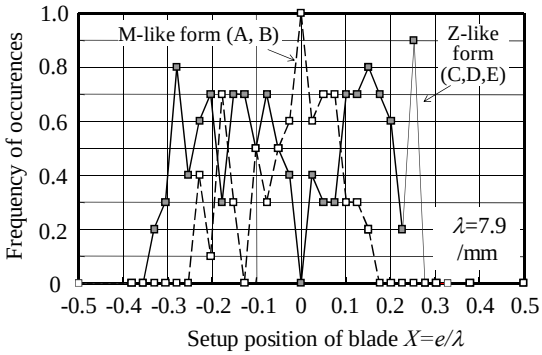

Fig.10 Distribution of large-grouped modes: Z-like and M-like crushing form with free condition

Table 3 Estimated probability p_i of representative modes for $|X|<0.5$

(a) Constraint: soft-fixing

Mode(+/-)	C	D	E	C,D,E	A,B	F,G
Prob. %	10.4	6.6	10.3	27.2	19.4	53.4

(b) Constraint: free

Mode(+/-)	C	D	E	C,D,E	A,B	F,G
Prob. %	6.1	7.5	14.5	28.0	16.3	55.7

As three modes C, D, E have the possibility for generating the string-like paper dust, the probability $p_{\{CDE\}}$ of the union mode {C,D,E} appears to be appropriate for watching the occurrence of string-like paper dust.

From Table 3, it was found that the balance of the probabilities p_C, p_E varied remarkably with the boundary constraint. Regarding generation of the string-like paper dust, the probabilities p_D, $p_{\{CDE\}}$ of the *free* condition were a little large, compared with those of the *soft-fixing* constraint.

According to the video data of the CM during blade indentation for d/t=0.5~0.8, it was found that, in case of the *free* condition, a shallow-crushed Z-like form gradually became a deep-crushed Z-like form, owing to the lateral (horizontal) sliding and the bend-up of Cpb. In the case of the *soft-fixing* constraint, it was observed that Mode C or E was not easily transformed to Mode D due to the constraint of Cpb.

In actual case of die-cutting process, as Cpb is fixed by a rubber-sponge rule, the crushing form of the CM appears to be affected by the setup condition of the rubber-sponge fixture. From the aspect of real-boundary constraint of Cpb, the probability of Z-like form must be furthermore investigated.

3.3 Estimation of asymmetric wave form of corrugated medium

The crushing form of the CM and the distribution of each mode with the setup position X were asymmetric as shown in Figs.7 to 10. The occurrence of M-like form (apex crushing) was apt to move on the right side with the origin of X=0. The neutral position of apex crushing was expected to lie in the range of $0<X<0.1$.

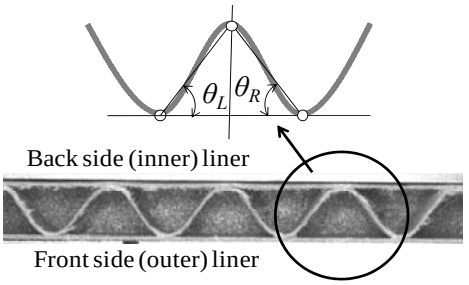

Fig.11 Measurement of inclined angles θ_L, θ_R

As such the eccentric occurrence of the crushing form of the CM appeared to be caused by the initial shape of the CM itself; geometrical profile of the CM was evaluated from photographs of a virgin specimen.

Fig.11 illustrates how to measure the inclined angles θ_L, θ_R of the CM. Through the

measurement of three apex nodes of the CM wave, the angles θ_L, θ_R were calculated for nine positions. Their maximum and minimum values were 51.1° and 46.5° respectively. The average difference between θ_R and θ_L measured was roughly 1° ($\theta_R \approx \theta_L$+1°).

In order to confirm the crushing stability of the CM, the flat crush test was applied to rectangle-formed specimens (as shown in Fig.1). 10 samples were examined with the feed velocity of 0.4 /mms^{-1}. From the result, two patterns were detected as shown in Fig.12: (a) 30% of the CM was tipped up on the left side; (b) 70% of the CM was upset in symmetry. There was a certain eccentricity of the CM form for the flat crush test [‡]. The occurrence of left side tipping-up appeared to be caused by the difference between the left-side and right-side in-plane stiffness of the CM, and also the difference between θ_L and θ_R. It seemed that the left side of the CM was easily buckled and eventually the apex points of the CM tended to move on the left side.

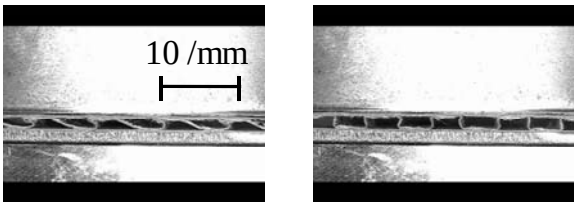

(a) Tipping up on the left (b) Symmetric upset

Fig.12 Flat crush test of rectangle-formed specimen (C-fluted board, Width: 10/mm, Length: 40/mm, Feed velocity:V=0.4/mms^{-1})

So far, it is concluded that there is correlation between the initial eccentricity of the CM form and the asymmetric distribution of the crushing modes' occurrence. In other words, if the occurrence frequency of several modes, such as Mode B and the union mode {C,D,E}, is measured with respect to X and if the distribution of the frequency is asymmetric, then the eccentricity of the initial CM form can be estimated from that correlation.

3.4 Cutting load response to crushing mode

Fig.13 shows the cutting load response on the final stage of d/t= 0.7~1.0 in the cases of X=0, 0.1 and 0.5. From Fig.13(a) and Fig.13(c), it was confirmed that the starting position, where the blade bit three pieces of compressed sheets, was $d/t \approx$ 0.87, while the load response of them was different for each other due to a difference of the stacked order of the outside liner, the CM, and the inside liner.

In the case of X= +0.1, three patterns of load response were actually detected. They were corresponded to Mode B+, C+ and D+ as shown in Fig.13 (b).

When the blade bites the Z-like form of the CM, the stacked thickness can be totally estimated as five times the raw-materials thickness. From Fig. 13 (b), as the starting position of Mode D+ was $d/t \approx$ 0.78, this position approximately corresponded to five times the raw-materials thickness. It was found that the load response of Mode C+ behaved as the middle state between D+ and B+. Since the occurrence position (d/t) of peaked-line force differed with respect to Mode D and B, it was found that it was possible to infer the pattern recognition of those deformation modes from the position (or the timing) of peaked load response, if appropriate sensors were implanted on the blade system[5].

‡This seems to be a reason why a circle-formed specimen is used for the standard flat crush test (JIS-Z0403-1).

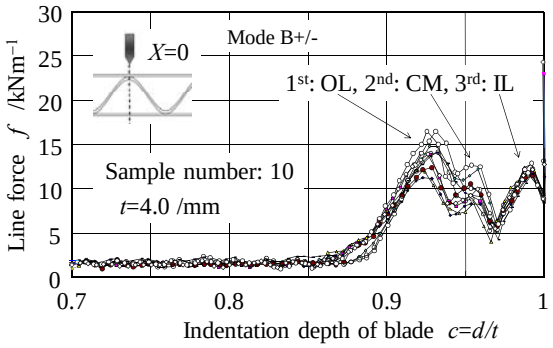

(a) In case of X=0, Mode B+/-

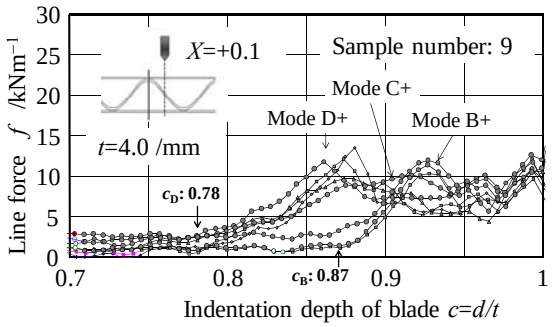

(b) In case of X=+0.1, Mode B+, C+, D+

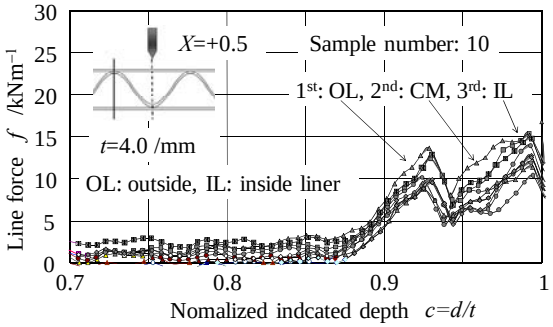

(c) In case of X=+0.5, Mode F+/-

Fig.13 Relationship between cutting line force and indentation depth of blade (in case of *free* condition)

4. Conclusions

A 42° center-bevel blade was quasi-statically indented to rectangle-formed specimen of heightwise corrugated paperboard (Cpb) by varying the setup position X of the blade, and the side view of Cpb was observed by using a CCD camera. Through this experiment, the followings were revealed.

(1) Deformation of the corrugated medium (CM) can be classified with three macro-grouped modes. It is also arranged with five kinds of actual crushing modes: B (cut off the apex), C (moved aside the Z-form due to insufficient folding), D (just cut off the Z-form), E (moved aside the Z-form due to surplus folding) and F (pushed the back-side liner and cut the root).

(2) Distribution of occurrence frequency of crushing form of the CM was varied with the boundary constraint of Cpb.

(3) In the *free* condition, the occurrence of Z-like form was apt to be promoted, as compared with the *soft-fixing* constraint.

(4) Proposed classification and pattern recognition of deformation mode of the CM are useful for estimating the initial-asymmetric structure of the CM.

(5) To monitor the load response is useful for detecting the deformation mode of the CM.

Acknowledgement

This work was supported by the JSPS Grants-in-Aid for Scientific Research, Creative and Pioneering Research (C) of Grant Number **22560106**.

References

1) S. Mizuguchi, (eds), Advanced Technology on Industrial Packaging and Transportation, Fuji Techno System, Tokyo, p.239(2002)

2) Tech-times (eds), Advanced Handbook for Processing of Papers and Boards, Tech-times, p.261 (1988)

3) The Middle Japan Technical Committee for Corrugated Board, Monthly PACK & BOX, 8 (2), p.8 (2005)
4) S. Nagae, S. Nagasawa, Y. Fukuzawa, A. Hine, I. Katayama, SOSEI-TO-KAKOU, 45 (524), 742 (2004)
5) S. Suzuki, Y. Fukuzawa, S. Nagasawa, I. Katayama, H. Iijima, SOSEI-TO-KAKOU, 46 (538), 1061 (2005)

（原稿受付　2011 年 3 月 2 日）
（審査受理　2011 年 6 月 15 日）

Corrugated paperboard の段筋方向押抜きにおける中芯変形挙動の観察

永澤　茂*†、藤倉　正俊*、福澤　康*、梶塚　孝士**

本研究は、Corrugated paperboard (Cpb) の押抜き加工における紙粉発生現象を扱っている。Cpb の押抜き過程で、中芯の折れ曲がる変形挙動がどのように発生するのかを明らかにできれば、糸状紙粉の発生頻度を予測できると考えられる。段筋方向に配置されたくさび刃が Cpb に対して押込まれるとき、中芯の折り重なり変形は、刃先と中芯の山波との相対的な位置関係に依存して発生すると考えられる。 そこで本研究では、C 段の Cpb 試験片に対して段筋方向に沿った直状の 42° くさび刃を押し込む実験を行い、 動画によって Cpb の側面を観察して中芯の変形挙動を解析した。

実験で段頂を基準にし左右半周期について刃先位置を変えて、中芯の変形挙動が推移する様子を明らかにした。中芯の変形挙動は、M 形(山頂付近)、Z 形(中芯の重ね折り)、W 形(谷底付近) の 3 つに大分類できた。さらに Z 形を細かく 3 つに細分して、帯状紙粉の発生機構を示すとともに、全体を 10 種類の変形様式に分けて整理した。また、試験片の拘束条件に依存して、中芯変形挙動が変化する現象を明らかにした。試験片の拘束条件を変えると段波の横方向の自由度の違いによって M 形、W 形の出現率が顕著に変化するとわかった。

キーワード: せん断、型抜き、中芯、刃位置、折り曲げ、加工